



Tailoring the structure of S-PEEK/PDMS proton conductive membranes through applied electric fields

D. Liu, M.Z. Yates*

Department of Chemical Engineering and Laboratory for Laser Energetics, University of Rochester, Rochester, NY 14627, United States

ARTICLE INFO

Article history:

Received 27 February 2008

Received in revised form 22 May 2008

Accepted 24 May 2008

Available online 5 June 2008

Keywords:

S-PEEK

PDMS

Electric field

Particle assembly

Fuel cell membrane

ABSTRACT

Composite membranes were formed composed of proton conductive sulfonated poly(ether ether ketone) (S-PEEK) particles dispersed in a non-proton conductive polymeric matrix, a cross-linked poly(dimethyl siloxane) (PDMS). The structure of the composites was controlled by applying electric fields to suspensions of S-PEEK particles in the liquid PDMS precursor, followed by thermally initiated cross-linking polymerization to fix the field-induced structure. The effects of the electric field on membrane structure, proton conductivity, methanol permeability, and water swelling were examined. Under certain conditions, the applied electric field induced the S-PEEK particles to form long chains across the liquid PDMS prepolymers. The degree of particle chaining was a function of the electric field frequency, magnitude, and application time. The S-PEEK particle chaining resulted in an improvement of the membrane conductivity, water uptake ability, and dimensional stability in comparison to membranes containing randomly distributed particles. The particle chaining also increased the methanol permeation across the composite membranes, but the selectivity of the membranes for protons over methanol increased sharply because the increase in proton conductivity was much larger relative to the methanol permeability increase. The membranes also display anisotropic swelling behavior in water that may prove advantageous for enhancing mechanical stability in fuel cells undergoing humidity cycling. The present study demonstrates a novel fabrication approach that can be used to control the structure of a variety of types of composite membranes to enhance performance for fuel cell applications.

© 2008 Elsevier B.V. All rights reserved.

1. Introduction

The drive to commercialize fuel cells for portable power, automotive applications, and stationary power sources has led to an increased interest in finding new types of proton-conducting membranes that can improve fuel cell performance and lower cost [1,2]. The principle of proton exchange membrane (PEM) fuel cell technology is the production of electricity by an electrochemical reaction, which involves the oxidation of the fuel at the anode, producing protons that are transported through a membrane to the cathode to react with oxygen forming water [2]. The membrane material must allow proton transport while acting as a barrier to avoid direct contact between fuel and oxygen. Proton-conducting polymeric membranes are attractive for use in fuel cells for portable power and automotive applications because they allow operation at low temperature and allow for lightweight fuel cell design [3,4].

The state of the art polymeric membranes are based on sulfonated perfluoropolymers such as Nafion® ionomers and related materials. Sulfonated perfluoropolymers are chosen because they provide good gas barrier properties, high proton conductivity, and are chemically stable [5,6]. However, some commercial applications of existing polymeric membranes are hampered by low proton conductivity at low relative humidity, high methanol permeability, and poor mechanical properties above 130 °C [7,8]. One route to possibly overcome some of these limitations is to develop composite membranes, where functional particles are added to improve membrane properties. Hygroscopic silica [9,10], proton-conducting metal phosphate [11], and methanol permeation barrier zeolite [12] have been dispersed in the ionomer matrix in an effort to improve the water content, proton-conductance, and resistance to methanol permeation in the membranes. The properties of these membranes greatly depend on the composite structure, which is influenced by the size, shape, concentration, orientation, and arrangement of the dispersed particles [9]. A high loading of particles is often required to improve the proton conductivity or to lower methanol permeability, but high particle loading can result in a loss of the mechanical stability of the composite membranes [13–15]. Control

* Corresponding author. Tel.: +1 585 273 2335.

E-mail address: myates@che.rochester.edu (M.Z. Yates).

of the distribution of proton-conducting particles inside composite membranes would offer a route to enhance membrane conductivity using much lower particle concentrations than would be required for randomly distributed particles.

One possible method to control the distribution of particles in composite membranes is by exploiting the response of particles suspended in a liquid to an applied electric field. When an electric field is applied to a suspension of particles, the particles may rotate, translate, or aggregate into chains because of torques and forces induced by the applied field. The magnitude of the forces acting on the particles depends on the conductive and dielectric properties of the particles and surrounding medium. Electric fields have been used to control the structure of particle suspensions for a number of different applications. For example, applied alternating current (AC) fields have been used to rotate and align polymer cholesteric liquid-crystal flakes dispersed in propylene carbonate [16]. The cholesteric liquid-crystal flakes have reflective coloration that depends upon the viewing angle. The control of flake orientation by the applied electric field is used to control the color of the suspension and has potential application in imaging. Another example is the rotation and alignment of rod-shaped molecular-sieve crystals suspended in fluorocarbon oil under direct current (DC) field [17]. The rod-shaped molecular sieve crystals were aligned in the direction of the applied field and deposited onto a surface to yield a nanoporous thin film with long-range alignment of the pore direction. Biological cells can be induced to aggregate and fuse when a suspension of cells is subjected to an appropriate electric field [18,19]. Spherical or irregular shaped dielectric particles can be induced to aggregate into chains that dramatically increase the apparent viscosity of the particle suspension. These types of suspensions are known as electrorheological fluids and have application in a number of devices [20,21]. Particle chaining phenomena have also been used to control the structure of composite ion-exchange membranes for electro-dialysis [22].

In the present study, we employed proton conductive sulfonated poly(ether ether ketone) (S-PEEK) particles and non-conductive cross-linked poly(dimethyl siloxane) (PDMS) polymer matrix to fabricate composite membranes under an electric field. The S-PEEK was chosen on the basis of easy processing from poly(ether ether ketone) (PEEK) [23] and because S-PEEK is promising as an alternative to Nafion® in PEM fuel cells [24]. PDMS was chosen as a model non-conducting matrix because liquid PDMS prepolymers can easily be converted to a cross-linked solid without the need to remove solvent. The structure of composite membranes was controlled by applying an electric field to a suspension of S-PEEK particles dispersed in a liquid PDMS prepolymer. The resulting structure was fixed by heating the prepolymer to form a solid cross-linked composite membrane.

2. Theoretical background: effects of electric fields on particles

The electric field voltage, application time, and frequency were varied to examine the effect on the structure, proton conductivity, methanol permeability, and dimensional stability of the composite membranes. When particles are suspended in dielectric solvents and exposed to an electric field, the applied field polarizes the particles along the field direction. Interactions between the field-induced dipole moment and external field cause particle migration to stronger or weaker field regions, which is known as dielectrophoresis (DEP) [25,26]. Mutual interactions of the induced dipole moments direct particles into assemblies such as “string of pearl” particle chains extending in the direction of the applied field. It is

the objective of the present study to assemble proton-conducting particles into chains that can act as transport paths.

Assuming particles are spheres with diameter d , dispersed in a dielectric fluid and exposed to an AC field E_{rms} , the time-average DEP force is given by Eq. (1):

$$\langle \bar{F}_{\text{DEP}} \rangle = 2\pi\epsilon_0\epsilon_1 \text{Re}[K(\omega)] \nabla E_{\text{rms}}^2 \left(\frac{d}{2}\right)^3 \quad (1)$$

where ϵ_0 , ϵ_1 , and ω are the permittivity of free space, relative permittivity of the solvent and angle frequency. $\text{Re}[K(\omega)]$ is the real part of the complex Clausius–Mossotti function defined in Eq. (2):

$$\text{Re}[K(\omega)] = \frac{\epsilon_2 - \epsilon_1}{\epsilon_2 + 2\epsilon_1} + \frac{3(\epsilon_1\sigma_2 - \epsilon_2\sigma_1)}{\tau_{\text{MW}}(\sigma_2 + 2\sigma_1)^2(1 + \omega^2\tau_{\text{MW}}^2)} \quad (2)$$

The Clausius–Mossotti function measures the effective polarizability of the particles, where ϵ_2 is the relative permittivity of the particles; σ_1 and σ_2 are conductivity of the solvent and particles; τ_{MW} is the Maxwell–Wagner charge relaxation time [26].

The mutual interaction force between particle i at the origin due to particle j located at (R_{ij}, θ_{ij}) in spherical coordinates is given by Eq. (3) [27]:

$$F_{ij}(R_{ij}, \theta_{ij}) = \frac{3}{16}\pi\epsilon_0\epsilon_1 \text{Re}[K(\omega)]^2 E_{\text{rms}}^2 \left(\frac{d^6}{R_{ij}^4}\right) \{ [3 \cos^2\theta_{ij} - 1]e_r + [\sin 2\theta_{ij}]e_\theta \} \quad (3)$$

where e_r and e_θ are the unit vectors in R and θ directions, respectively. E_{rms} is the root-mean-square (rms) electric field. From Eqs. (1) and (3), it can be seen that the DEP and mutual interaction forces are controlled primarily by either the conductivities or permittivities of the system, depending on the field frequency. In the lower frequency range ($\omega \rightarrow 0$), the conductivity of particles and solvent controls the interaction forces. While in the higher frequency range ($\omega \rightarrow \infty$), the permittivities of the particles and solvent dominate the response. The transition from the conductivity-controlled response to the permittivity-controlled response occurs at the critical frequency, f_c [28]:

$$f_c = \frac{\sigma_2 + 2\sigma_1}{2\pi(\epsilon_2 + 2\epsilon_1)\epsilon_0} \quad (4)$$

For particle chaining to occur, the DEP and mutual interaction forces must be strong enough to overwhelm the hydrodynamic, Brownian or other colloidal forces that act to disrupt the field-induced structure [27,29]. A higher field strength is thus preferable to achieve particle chaining. However, the maximum practical field strength is limited by electric breakdown and Joule heating that both act to destroy the material or disrupt the particle chaining [30,31].

The time for a chain of n particles to form can be predicated by the following equation [32]:

$$t'(n) \propto \left(\sum_{i=1}^n (2^3)^{i-1} \right) \left(\frac{3\pi\eta d}{E_{\text{rms}}^2} \right) \left(\frac{l'^5}{d^6} \right) \quad (5)$$

where l' is the distance of separation between particles, η is the liquid viscosity, and all other parameters are as defined above. From Eq. (5), it can be seen that the time required to form particle chains increases with increasing solvent viscosity and decreases with increasing field strength. The time required for chaining is also strongly dependent on particle size, with larger particles forming chains more rapidly than smaller particles. In the present study, long particle chains completely spanning the membranes are required for proton conduction.

3. Experimental

3.1. Materials

The PDMS prepolymer (Sylgard® 182) was purchased from Dow Corning®. PEEK was purchased from Polysciences, Inc. S-PEEK was obtained by sulfonation of PEEK following a reported procedure [23]. The sulfonation reaction was conducted in concentrated (95–98%) sulfuric acid under vigorous stirring at room temperature for 2 days to obtain partially sulfonated PEEK with IEC value of 1.54 mequiv./g. The resulting IEC value indicates a 53% degree of sulfonation [23]. Fully sulfonated PEEK was not used because it loses mechanical stability when exposed to water [33]. The partially sulfonated S-PEEK was precipitated by adding its solution dropwise into a large excess of ice-cold water under mechanical agitation. The S-PEEK precipitate was then left to settle overnight, filtered, washed with deionized water and dried in a vacuum oven overnight at 100 °C. Finally, the dry S-PEEK was ground with a pestle and mortar and then sieved to produce smaller sized particles (<45 μm).

3.2. Membrane formation

Weighed amounts of S-PEEK particles and PDMS prepolymers were mixed thoroughly with a Vortex-Genie™ (Scientific Industries, INC.). Then, the mixture was subjected to a vacuum oven at room temperature for 30 min to release air bubbles trapped in the mixture. The S-PEEK suspension was then transferred to one of two molds shown in Fig. 1 that incorporate electrodes. To align S-PEEK particles in-plane and through-plane directions in the PDMS polymeric matrix, two different membrane molds were constructed, as shown in Fig. 1a and b. In Fig. 1a, the cell consists of a glass substrate (25 mm × 75 mm × 70 mm) used to separate the two aluminum (Al) electrodes that are connected to the power source. A Mylar frame (24 mm × 25 mm × 0.1 mm) is placed on top of the glass substrate as a mold for holding the film of the liquid PDMS precursor with dispersed S-PEEK particles. A field applied across the aluminum electrodes acts to direct particle alignment in the plane of the thin PDMS film. Fig. 1b shows the mold for preparation of membranes with through-plane aligned particles. The cell contains two pieces of indium tin oxide (ITO)-coated glass slides with size of 50 mm × 50 mm × 1.1 mm as the electrodes. The ITO coated sides of the two electrodes are arranged to face each other and a Teflon frame (25 mm × 25 mm × 0.381 mm) is a spacer to separate the two ITO coated slides and hold the suspension of S-PEEK particles in the liquid PDMS polymer precursor. The power source consisted of a 20 MHz Function/Arbitrary Waveform Generator (Agilent 33220A, Agilent Technologies) to provide DC or AC signal, a high-voltage power amplifier (Model 10/10B, Trek, Inc.) to amplify the voltage of

the AC or DC input signal by a factor of 1000, and a 20 MHz dual trace oscilloscope (Model 72-6800, Tenma Test Equipment) to monitor the output voltage and current signal. After applying the field either through the thin film or in the plane of the thin film, the electrode cells were heated to 100 °C on a hot plate to thermally cure the PDMS. During curing, the EF was continuously applied for 5 min. After that, the field was stopped and the membrane was put into the oven at 100 °C for 40 min to complete curing. For control membranes formed without an applied field, the cell shown in Fig. 1a was used and the same procedure followed except the cell holding the membranes was directly placed in an oven at 100 °C for 45 min to cure the PDMS.

3.3. Membrane characterization

Direct observation of the S-PEEK particle movement under an EF was carried out using an inverted phase contrast optical microscope (TC5000, Meiji Techno Co., Ltd.) equipped with a digital camera. The particle chaining across the PDMS matrix under an EF was further verified with the microscope after the composite membrane was cured. Proton conductivity of the membranes was determined using a Solartron Instrument 1260 Impedance/Gain-phase analyzer over a frequency range of 32 MHz to 0.1 Hz. The membranes (11 mm wide and 20 mm long) were placed in a conductivity cell (Bek-Tech LLC) with two platinum mesh probes (2 mm wide) used for impedance scanning along the S-PEEK particle chaining direction. Prior to the conductivity measurement, all membranes were pre-hydrated in deionized water for at least 10 days to reach saturation. Then, the humidified membrane was taken out and excess water at the surface was swept away with tissue paper. The membrane was enclosed in the sample holder and the measurement was conducted immediately. The whole process took around 3 min from the time the membrane was initially removed from water. It was assumed that the membrane remained saturated with water during the measurement. All measurements were done under room temperature. The membrane resistance R was determined by extrapolating the complex impedance spectroscopy at a high frequency arc to the real axis. The proton conductivity was calculated from the equation $\sigma = l/(R \cdot A)$, where σ is the proton conductivity, l the distance between two outer electrodes and A is the cross-section area of the membrane.

The water uptake of the composite membranes was measured by immersing the dry membranes (dried at 70 °C in a vacuum oven for 24 h) into deionized water and weighing periodically until the membrane reached a constant weight. Dimensional changes were measured by using a micrometer to directly measure the dry and wet membrane area and thickness immediately after their corresponding weight measurements.

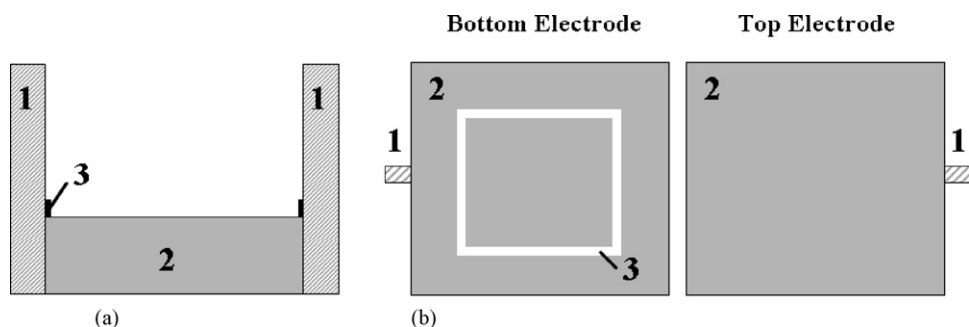


Fig. 1. Schematic view of the cell used for preparation of ordered PEEK/PDMS composite membranes under an electric field. (a) Side-view of the set-up for S-PEEK in-plane alignment (1, Aluminum electrode; 2, Glass substrate; 3, Mylar frame). (b) Top view of the set-up for S-PEEK through-plane alignment (1, Aluminum foil; 2, ITO coated glass slide; 3, Teflon frame).

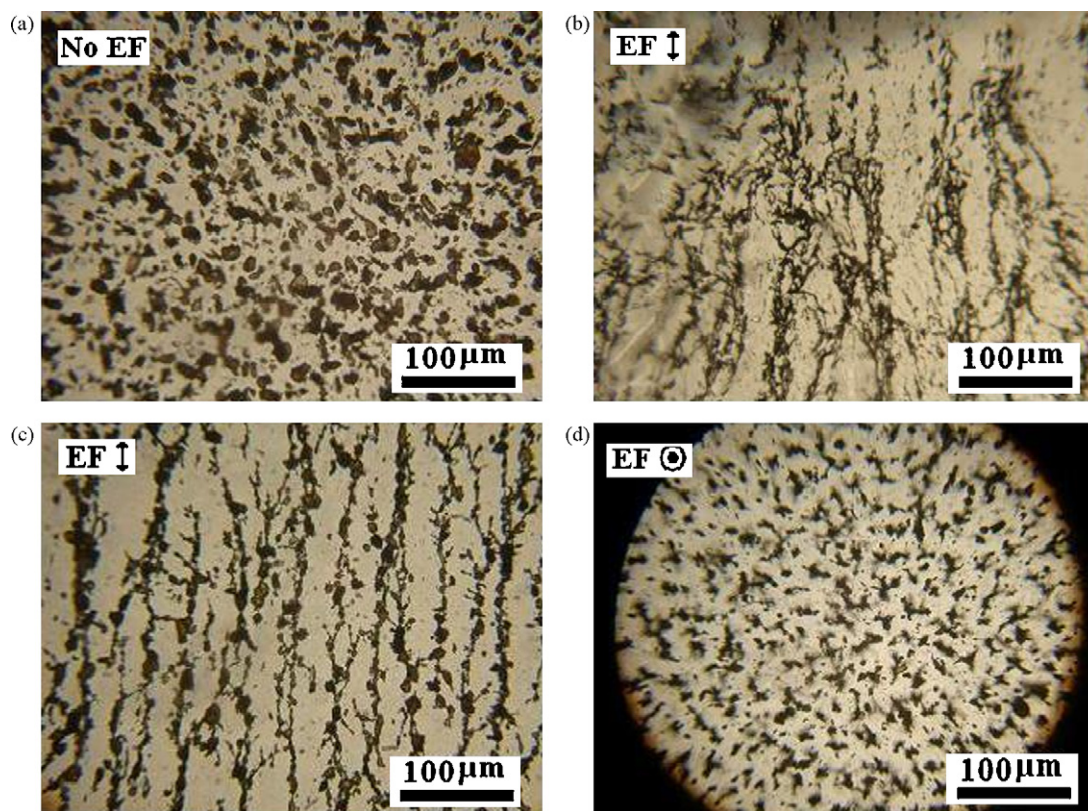


Fig. 2. Optical microscopy images of S-PEEK particles in PDMS membranes: (a) non-aligned; (b) in-plane aligned under DC field; (c) in-plane aligned under AC field; (d) through-plane aligned under AC field.

Methanol permeability of membranes was investigated using gas chromatography (GC, HP model 8590A) with a capillary column (Agilent Co., 30 m \times 0.32 mm \times 0.50 μ m, DB-Wax) and a FID detector to measure methanol permeate concentration. The membrane was clamped between two 30 ml reservoirs using a custom made glass permeability cell. One side of the membrane was exposed to a 3 M methanol/water solution and the other side was exposed to pure deionized water. The apparatus was kept at room temperature (\sim 26 $^{\circ}$ C) under magnetic stirring at rate of 1200 rpm. The methanol permeability was determined from the concentration of methanol versus time on the side of the membrane originally containing pure water by using an approximate solution of the continuity equation for diffusion in plane sheet geometry at early times [34,35].

4. Results and discussion

4.1. S-PEEK particle chaining under DC/AC field

The initial analysis of particle chaining induced by the applied electric field was conducted through the optical microscopy of cured composite membranes. A low amount of S-PEEK particles (5 wt%) was used in these experiments to allow viewing of individual particle chains. Fig. 2a–d show images of the membranes prepared under no applied field, a DC field with in-plane alignment, an AC field with in-plane alignment, and AC field with through-plane alignment. S-PEEK particles distributed randomly and uniformly inside the PDMS polymer matrix before the electric field was applied, as shown in Fig. 2a. When a DC field with strength of 282.8 V/mm was applied for 10 min, S-PEEK particles aggregated into chains, as shown in Fig. 2b. Under a DC field, the particle chain structure was disrupted in regions near the cathode due to the electrophoresis force acting to repel the negatively

charged particle chains from the negative electrode. Electrophoresis can be eliminated by application of an AC field. Fig. 2c shows the resulting composite structure when an AC field of $V_{\text{rms}} = 100$ V/mm ($V_{\text{pp}} = 282.8$ V/mm) and $f = 25$ Hz was applied for the same time as the DC field. The AC field results in continuous and uniform particle chains that bridge the gap from the anode to the cathode. Fig. 2d shows the particle chains aligned in the through-plane direction of the membranes using the same AC field strength and time as used in Fig. 2c.

Considering that the S-PEEK particles are proton conductive and are dispersed in a non-conductive PDMS matrix, the conductivity of the composite membranes should be strongly affected by the S-PEEK particle distribution inside the membrane. The electric field induced S-PEEK particle chaining provides proton-conducting pathways inside the composite membranes. As a result, the proton conductivity of the composite membranes is improved by the field-induced structure that is formed. The proton conductivity of the membranes prepared under no applied field, DC and AC field, were measured for composites containing 14 wt% S-PEEK particles. These membranes used for proton conductivity measurement were formed under the same conditions as the samples in Fig. 2; only the S-PEEK concentration was increased. Without an applied field, the proton conductivity is very low (3.38×10^{-8} S/cm). The membrane formed under the DC field has an improved conductivity of 7.47×10^{-7} S/cm, while the composite membrane prepared under AC field has the highest conductivity of 8.74×10^{-5} S/cm. This trend in proton conductivity corresponds to the degree of particle chaining in the membranes prepared under the three different conditions: no applied field, DC field and AC field. Without the electric field, particles are randomly distributed. The DC field induces chains to form, but the chains are not uniform across the membrane. The S-PEEK particles are negatively charged due to

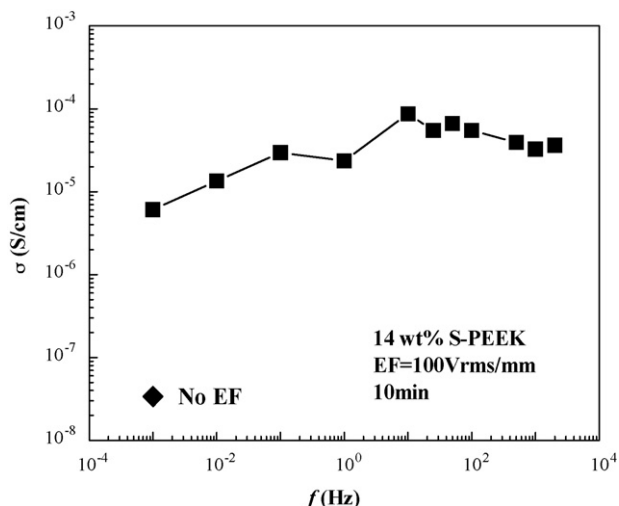


Fig. 3. Membrane conductivity as a function of applied field frequency.

sulfate groups. As a result, electrophoresis results in S-PEEK particle accumulation near the anode and depletion near the cathode. The AC field effectively eliminates particle electrophoresis, allowing more uniform distribution of particles and chains through the membrane to improve the membrane proton conductivity. Considering this result, AC fields were used exclusively for particle chaining and conductivity improvement in the remainder of this study.

4.2. The effect of AC field frequency

For the study of the field frequency effect, all of the membranes were prepared under fixed field strength of 100 V_{rms}/mm , field application time of 10 min and S-PEEK content of 14 wt%. The particles were aligned in-plane direction of the membranes under various frequencies ranging from 1 mHz to 2 kHz. Fig. 3 shows the proton conductivity of the prepared composite membranes measured along the particle alignment direction. For the membrane prepared under the lowest frequency of 1 mHz, the proton conductivity is low ($\sim 6.06 \times 10^{-6}$ S/cm), but it is still higher than that of the membrane with randomly distributed particles (3.38×10^{-8} S/cm). The proton conductivity of the membranes is increased to 8.74×10^{-5} S/cm when the field frequency is increased to 10 Hz. From 10 to 100 Hz, the conductivity appears to reach a plateau value. Further increase of the frequency to 2 kHz is not helpful for increasing the proton conductivity. In fact, the conductivity decreases slightly in the high frequency range. Two kilohertz is the maximum frequency that could be applied at a field strength of 100 V_{rms}/mm due to the limitations of the power amplifier.

It is known that DEP and mutual interaction forces are dominated by conductivity mismatch at low frequency or permittivity mismatch at high frequency of the system [28]. The transition from conductivity-controlled response at low frequency to permittivity-controlled response at high frequency occurs at the frequency f_c . The conductivity of non-hydrated S-PEEK (σ_2) particles is $\sim 10^{-6}$ S/cm, which is much higher than that of non-conductive silicone elastomer with conductivity of $\sigma_1 \sim 10^{-16}$ S/cm [36]. The measurement on dielectric properties of S-PEEK and PDMS showed that S-PEEK has a higher dielectric constant ($\epsilon_2 = 158$ at 10,000 Hz) than that of PDMS ($\epsilon_1 = 2.49$ at 10,000 Hz). The conductivity mismatch between the S-PEEK and PDMS is relatively large compared to the permittivity mismatch and f_c is around 100,000 Hz. In the studied frequency range of 1 mHz to 2 kHz, the conductivity mis-

match always exists and dominates particle chaining. As a result, the conductivity of the membranes is improved by the applied electric field under the entire frequency range studied. When the frequency is above 1 kHz, the proton conductivity does not improve as much as with lower frequencies. One probable reason is that DEP and mutual interaction forces are smaller at higher frequencies since free charges do not have sufficient time to migrate, which causes a decrease in the effective particle polarizability. At very low frequencies, proton conductivity is not improved greatly due to electrophoresis of the particle chains. Therefore, the optimal frequency range for particle chaining in this system is in the medium frequency range from 10 to 100 Hz.

4.3. The effect of AC field strength

Fig. 4 shows the influence of field strength on the proton conductivity of the prepared composite membranes. In this study, all membranes were formed under the frequency of 25 Hz, application time of 10 min and S-PEEK concentration of 14 wt%. The field strength was varied from 1.4 to 140 V_{rms}/mm . Fig. 4 shows that the conductivity of the membrane increases with increasing field strength from 0 to 50 V_{rms}/mm . When the field strength is increased to 100 V_{rms}/mm , the conductivity of the membrane starts to reach a plateau. Further increase the field strength above 100 V_{rms}/mm does not significantly change the proton conductivity. This data indicate that the minimum field strength required for particle chaining to dominate after the 10 min is around 100 V_{rms}/mm . It is possible that the minimum field strength could be further reduced by increasing the application time, since time and field strength are inversely related as shown in Eq. (5).

4.4. The effect of AC field application time

To study the minimum time required for the formation of the long particle chains spanning the membrane, a range of times from 0.5 to 120 min were examined as the field frequency, strength and S-PEEK concentration were held to 100 V_{rms}/mm , 25 Hz and 14 wt%, respectively. Again, the proton conductivity was employed as a measure of the effectiveness of particle chaining, as shown in Fig. 5. From this figure, we can see that with increasing time, the degree of particle chaining increased. After approximately 7 min, the conductivity reaches a plateau. Further increase of the application time to 120 min does not significantly change conductivity. This result

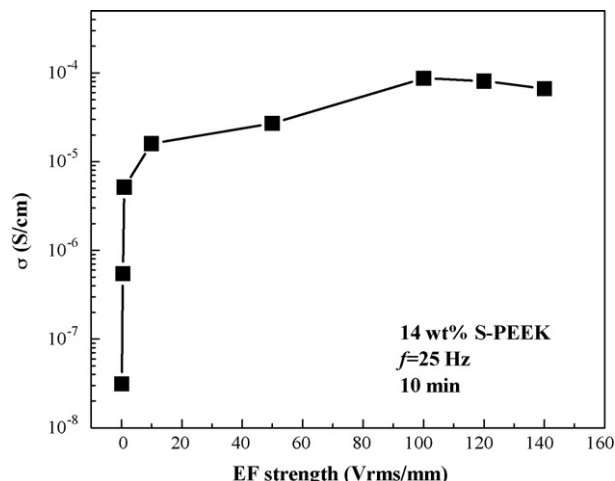


Fig. 4. Membrane conductivity as a function of the applied field strength.

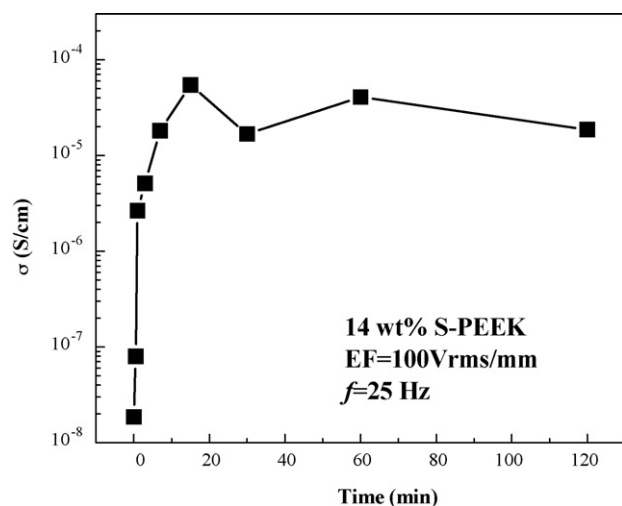


Fig. 5. Membrane conductivity as a function of field application time.

shows that a time of at least 7 min is required for conductivity improvement in the composite membranes formed under a field strength of 100 V_{rms} /mm. Shorter times could possibly be used at higher field strength, as suggested by Eq. (5).

4.5. Proton conductivity versus particle concentration

The effect of the applied electric field on the proton conductivity of a series of membranes with varying S-PEEK particle concentration is shown in Fig. 6. An AC field of 100 V_{rms} /mm and 25 Hz was applied for 10 min for all samples. When the S-PEEK particle concentration is low such as 5 wt%, there is no obvious improvement of the proton conductivity for membranes formed under the electric field as compared to membranes formed without the applied field. This is due to the low particle number that is not enough to form continuous channels for proton transport from one side of the membrane to the other side. With increasing particle concentration to 10 wt%, the proton conductivity is obviously improved as the conductivity is ~ 1000 times higher for the membrane formed under the applied AC field than for the membrane prepared without the applied field. Further increase of the S-PEEK particle concentration also increases the conductivity, but the degree of improvement is

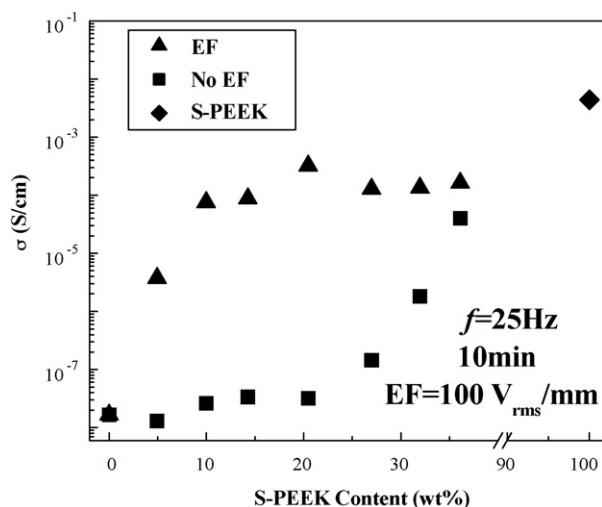


Fig. 6. Membrane conductivity as a function of S-PEEK content in the aligned and non-aligned composite membranes.

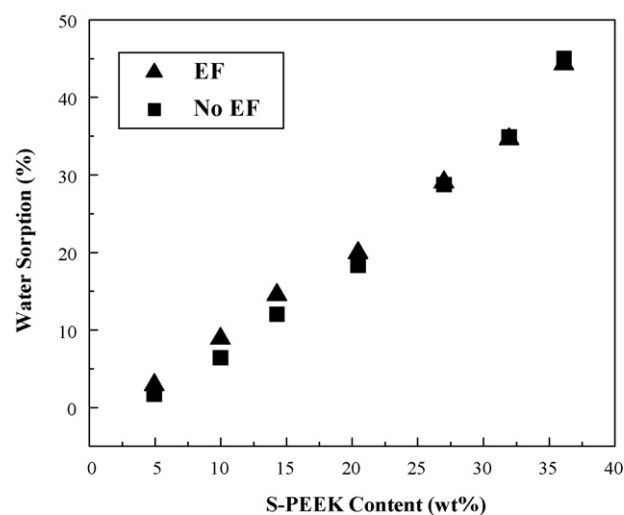


Fig. 7. Water sorption as function of the S-PEEK concentration in the aligned and non-aligned composite membranes.

small. The proton conductivity of the membranes formed under the electric field is increased by a factor of ~ 2 as the S-PEEK content increased from 10 to 40 wt%.

When the S-PEEK particle concentration is above 30 wt%, the membranes prepared without the application of the electric field begin to show significant increase in the proton conductivity. This is because the concentration is close to the percolation threshold of the membrane. Above the percolation threshold, the randomly distributed particles begin to form an interconnected network that provides conduction pathways through the membrane. As particle concentration is increased, membranes formed with and without an applied field display similar conductivities as the percolation threshold is exceeded. Obviously, the structure induced by the applied field causes the percolation threshold to be reduced. This data illustrates an approach to fabricate conductive composite membranes with lower particle content than would be required to achieve the same conductivity with randomly distributed particles. The composite membranes with randomly distributed particles require a high particle loading to improve the conductivity of the membrane. High particle loading usually deteriorates the mechanical stability of composite membranes, so the electric field-induced structure is a promising route to create composite membranes that maintain good mechanical properties by providing high conductivity at low particle concentration.

4.6. Water sorption

Water sorption at room temperature was measured for the series of membranes used in Fig. 6. The water uptake increases with increasing particle content in the both aligned and non-aligned composites membranes, as shown in Fig. 7. Since PDMS is hydrophobic, all of the absorbed water is from the S-PEEK particles. With low concentrations of S-PEEK, the membranes with aligned particles have slightly higher water sorption than that of non-aligned membranes. However, as the concentration of S-PEEK is increased, the water sorption of the two types of membranes approaches a similar value. This is due to the formation of good connectivity of particles inside the polymer matrix when a high particle concentration is employed. The water uptake is consistent with the proton conductivity enhancement of the composite membranes shown in Fig. 6.

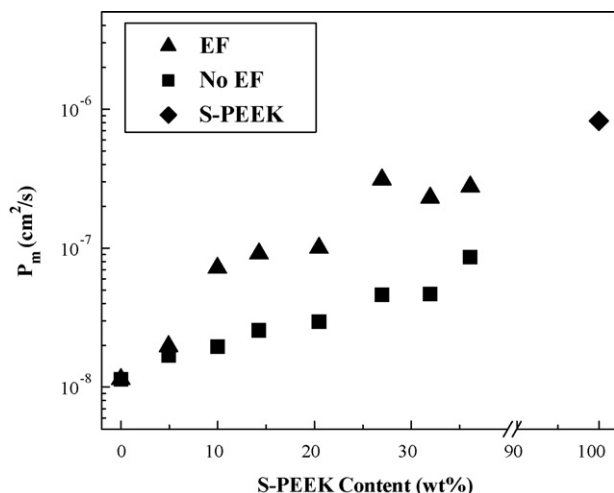


Fig. 8. Methanol permeability as a function of the S-PEEK concentration in the aligned and non-aligned composite membranes.

4.7. Methanol permeability and membrane selectivity

The dependence of the S-PEEK particle chaining on the methanol permeability through the PDMS membranes is shown in Fig. 8. The methanol permeability increases with increasing S-PEEK content in the composite membranes comprised of chained and non-chained particles. For the composite membranes containing the same amount of S-PEEK, the membranes prepared under the electric field have increased methanol permeability. This can be easily understood from the proton conductivity data since the connectivity of particles in chains provides transport pathways for both protons and methanol. With the measured proton conductivity and methanol permeability results, the selectivity (α) of the composite membranes for protons over methanol can be defined as the proton conductivity divided by the methanol permeability [12,35]. Fig. 9 illustrates the membrane selectivity of the composite membranes fabricated with and without an applied electric field. The composite membranes formed under an electric field have an enhanced selectivity at particle concentrations below the percolation threshold for conductivity. At some concentrations below the percolation threshold, there is an enhancement in proton conductivity of ~1000 times

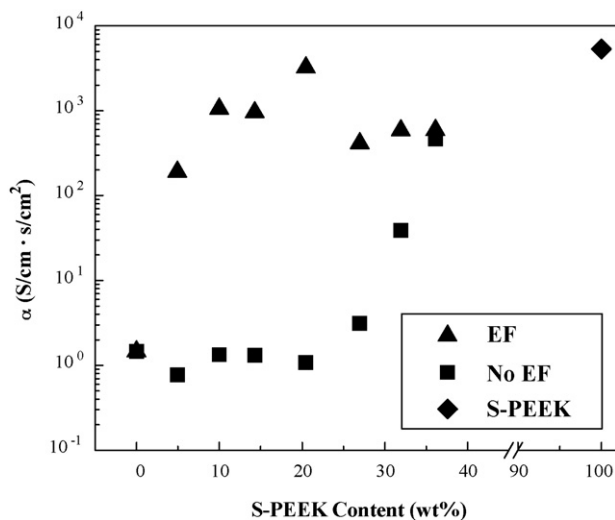


Fig. 9. Selectivity as a function of the S-PEEK content in the aligned and non-aligned composite membranes.

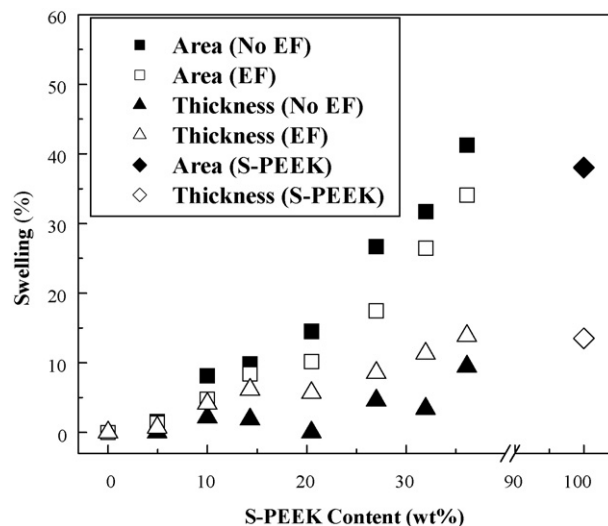


Fig. 10. Dimensional stability as a function of the S-PEEK concentration in the aligned and non-aligned composite membranes.

while the methanol permeability increases only ~20 times for membranes with particles aligned under an applied field compared to disordered membranes. The differences in membrane selectivity between composite membranes with aligned and non-aligned particles are reduced after the particles reach the percolation concentration. The reduced methanol permeation in comparison with protons through the membranes may be due to the suppressed swelling of S-PEEK phase in the PDMS matrix. Previous have shown a reduction in methanol permeation when polymer gels were confined in pores to limit swelling [37,38].

4.8. Dimensional stability

The membrane dimensional stability was characterized by the changes in the membrane area and thickness between the dry and water swollen states. Fig. 10 shows the dimensional changes measured for composite membranes prepared under the applied field compared with disordered membranes. In Fig. 10, the area and thickness expansion both are increased with increasing S-PEEK concentration in composite membranes with aligned and non-aligned particles. However, for membranes with the same particle content, the area expansion is reduced when the S-PEEK particles are aligned in chains, while the thickness expansion is increased. This indicates that the membrane swelling is anisotropic for the membranes with aligned particles. The swelling is enhanced in the direction of particle alignment. The dimensional stability under water swelling is important for practical operation proton-conducting membranes used in fuel cells, and especially so under humidity cycling. The fuel cell electrode can detach from a membrane due to stress from the change in membrane area upon swelling with water [37]. The composite membranes containing chained particles fabricated in the present approach can effectively reduce the membrane area expansion, which is promising for the membrane application in fuel cells as a route to enhance mechanical stability of membrane/electrode assemblies under humidity cycling during fuel cell operation.

5. Conclusions

Electric field-directed particle assembly shows promise as a route to control the structure of polymer composite proton exchange membranes to improve performance in fuel cells.

The field-induced structure can be adjusted to balance proton conductivity, methanol permeability, membrane selectivity and mechanical stability. The application of AC electric fields results in the aggregation of proton-conducting particles into long particle chains spanning the thickness of composite polymer membranes. The particle chains act as proton conductive channels through the membranes. Particle chaining was controlled by electric field magnitude, frequency, and application time. The field induced structure results in a reduction in the percolation threshold for ion-conductance in the direction of the particle chains. The amount of particles required to create conductive composites was reduced to around one third of that needed for membranes with randomly distributed particles. The membranes display anisotropic swelling behavior in water that may prove advantageous in fuel cell applications by reducing electrode delamination under humidity cycling. The membrane selectivity for protons over methanol was increased by particle chaining due to the matrix suppressed swelling of S-PEEK.

It should be noted that the S-PEEK/PDMS membranes themselves are not suitable for fuel cell application. The partially sulfonated S-PEEK does not have high enough proton conductivity and the PDMS support matrix has high oxygen permeability that would result in poor fuel cell performance. However, the membranes prepared in this study demonstrate the potential of the electric field processing technique to improve performance of fuel cell membranes. The electric field processing technique can be applied to support matrices with higher chemical stability and oxygen/fuel barrier properties and to particles with higher proton conductivity to improve fuel cell performance.

Acknowledgments

We acknowledge support from the DOE (DE-FG02-05ER15722) and the DOE through the Laboratory for Laser Energetics (DE-FC03-92SF19460) for support of this research.

Nomenclature

A	cross-section area of the membrane (cm^2)
d	particle diameter (m)
e_r	unit vector in R direction in spherical coordinates (m)
e_θ	unit vector in θ direction in spherical coordinates ($^\circ$)
E_{rms}	root mean square field strength (V/m)
∇E_{rms}	electric field gradient (V/m^2)
f_c	critical frequency (Hz)
i, j	position of spheres
l	distance between two outer electrodes (cm)
l'	distance of separation between particles (m)
n	number of particles
R	membrane resistance (Ω)
R_{ij}	radial distance from the origin i to j in spherical coordinates (m)
$\text{Re}[K(\omega)]$	real part of the complex Clausius–Mossotti function
t'	time for a pair of particles to meet (s)
t'_n	time for a chain of n particles to form (s)
Greek letters	
α	membrane selectivity ($\text{S}/\text{cm s}/\text{cm}^2$)
ϵ_0	permittivity of free space (F/m)
ϵ_1	relative permittivity of the solvent
ϵ_2	relative permittivity of the particle

η	solvent viscosity (Pa s)
θ_{ij}	angle from the origin i to j in spherical coordinates ($^\circ$)
σ	proton conductivity (S/cm)
σ_1	conductivity of the solvent (S/m)
σ_2	conductivity of the particle (S/m)
τ_{MW}	Maxwell–Wagner charge relaxation time (s)
ω	angle frequency (Hz)

References

- [1] L. Carrette, K.A. Friedrich, U. Stimming, Fuel cells: principles, types, fuels, and applications, Chem. Phys. Chem. 1 (2000) 162.
- [2] S.M. Haile, Fuel cell materials and components, Acta Mater. 51 (2003) 5981.
- [3] P. Costamagna, S. Srinivasan, Quantum jumps in the PEMFC science and technology from the 1960s to the year 2000. Part I. Fundamental scientific aspects, J. Power Sources 102 (2001) 242.
- [4] P. Costamagna, S. Srinivasan, Quantum jumps in the PEMFC science and technology from the 1960s to the year 2000. Part II. Engineering, technology development and application aspects, J. Power Sources 102 (2001) 253.
- [5] J.A. Kerres, Development of ionomer membranes for fuel cells, J. Membr. Sci. 185 (2001) 3.
- [6] W.G. Grot, Perfluorinated ion-exchange polymers and their use in research and industry, Macromol. Symp. 82 (1994) 161.
- [7] G. Alberti, M. Casciola, L. Massinelli, B. Bauer, Polymeric proton conducting membranes for medium temperature fuel cells (110–160 $^\circ\text{C}$), J. Membr. Sci. 185 (2001) 73.
- [8] J. Ling, O. Savadogo, Comparison of methanol crossover among four types of Nafion membranes, J. Electrochem. Soc. 151 (2004) A1604.
- [9] G. Alberti, M. Casciola, Composite membranes for medium-temperature PEM fuel cells, Annu. Rev. Mater. Res. 33 (2003) 129.
- [10] P. Staiti, A.S. Arico, V. Baglio, F. Lufrano, E. Passalacqua, V. Antonucci, Hybrid Nafion-silica membranes doped with heteropolyacids for application in direct methanol fuel cells, Solid State Ionics 145 (2001) 101.
- [11] C. Yang, S. Srinivasan, A.S. Arico, P. Creti, V. Baglio, V. Antonucci, Composite Nafion/Zirconium phosphate membranes for direct methanol fuel cell operation at high temperature, Electrochem. Solid State Lett. 4 (2001) A31.
- [12] B. Libby, W.H. Smyrl, E.L. Cussler, Polymer-Zeolite composite membranes for direct methanol fuel cells, AIChE J. 49 (2003) 991.
- [13] A.M. Herring, Inorganic-polymer composite membranes for proton exchange membrane fuel cells, Polym. Rev. 46 (2006) 245.
- [14] Z. Poltarzewski, W. Wieczorek, J. Przyłuski, V. Antonucci, Novel proton conducting composite electrolytes for application in methanol fuel cells, Solid State Ionics 119 (1999) 301.
- [15] M. Casciola, G. Alberti, A. Ciarletta, A. Cruccolini, P. Piaggio, M. Pica, Nanocomposite membranes made of zirconium phosphate sulfophenylphosphonate dispersed in polyvinylidene fluoride: preparation and proton conductivity, Solid State Ionics 176 (2005) 2985.
- [16] A. Trajkovska-Petkoska, R. Varshneya, T.Z. Kosc, K.L. Marshall, S.D. Jacobs, Enhanced electro-optic behavior for shaped polymer cholesteric liquid-crystal flakes made using soft lithography, Adv. Funct. Mater. 15 (2005) 217.
- [17] J.-C. Lin, M.Z. Yates, A. Trajkovska-Petkoska, S.D. Jacobs, Electric-field-driven assembly of oriented molecular-sieve films, Adv. Mater. 16 (2004) 1944.
- [18] U. Zimmermann, P. Scheurich, G. Pilwat, R. Benz, Cells with manipulated functions: new perspectives for cell biology, medicine, and technology, Angew. Chem. Int. Ed. Engl. 20 (1981) 325.
- [19] B. Alp, G.M. Stephens, G.H. Markx, Formation of artificial, structured microbial consortia (ASMC) by dielectrophoresis, Enzyme Microb. Technol. 31 (2002) 35.
- [20] P.J. Burke, Nano-dielectrophoresis: Electronic Nanotweezers, American Scientific Publishers, 2004.
- [21] T.C. Halsey, J.E. Martin, Electrorheological fluids, Sci. Am. 269 (1993) 58.
- [22] Y. Oren, V. Freger, C. Linder, Highly conductive ordered heterogeneous ion-exchange membranes, J. Membr. Sci. 239 (2004) 17.
- [23] S.M.J. Zaidi, S.D. Mikhailenko, G.P. Robertson, M.D. Guiver, S. Kaliaguine, Proton conducting composite membranes from polyether ether ketone and heteropolyacids for fuel cell applications, J. Membr. Sci. 173 (2000) 17.
- [24] R. Jiang, H.R. Kunz, J.M. Fenton, Investigation of membrane property and fuel cell behavior with sulfonated poly(ether ether ketone) electrolyte: temperature and relative humidity effects, J. Power Sources 150 (2005) 120.
- [25] H.A. Pohl, Dielectrophoresis, Cambridge University Press, Cambridge, UK, 1978.
- [26] T.B. Jones, Electromechanics of Particles, Cambridge University Press, Cambridge, UK, 1995.
- [27] M. Parthasarathy, D.J. Klingenberg, Electrorheology: mechanisms and models, Mater. Sci. Eng. R 17 (1996) 57.
- [28] B. Liu, M.T. Shaw, Electrorheology of filled silicone elastomers, J. Rheol. 45 (2001) 641.
- [29] A.P. Gast, C.F. Zukoski, Electrorheological fluids as colloidal suspensions, Adv. Coll. Interface Sci. 30 (1989) 153.

- [30] H. Morgan, N.G. Green, *AC Electrokinetics: Colloids and Nanoparticles*, Research Studies Press Ltd., Baldock, Hertfordshire, England, 2003.
- [31] T. Heida, *Electric Field-induced Effects on Neuronal Cell Biology Accompanying Dielectrophoretic Trapping*, Springer, 2003.
- [32] C. Park, R.E. Robertson, Alignment of particles by an electric field, *Mater. Sci. Eng. A-Struct.* 257 (1998) 295.
- [33] V.S. Silva, B. Ruffmann, H. Silva, Y.A. Gallego, A. Mendes, L.M. Madeira, S.P. Nunes, Proton electrolyte membrane properties and direct methanol fuel cell performance. I. Characterization of hybrid sulfonated poly(ether ether ketone)/zirconium oxide membranes, *J. Power Sources* 140 (2005) 34.
- [34] J. Crank, *The Mathematics of Diffusion*, Oxford University Press, Oxford, 1975.
- [35] Y.A. Elabd, E. Napadensky, J.M. Sloan, D.M. Crawford, C.W. Walker, Triblock copolymer ionomer membranes. Part I. Methanol and proton transport, *J. Membr. Sci.* 217 (2003) 227.
- [36] J.E. Mark, *Polymer Data Handbook*, Oxford University Press, New York, 1999.
- [37] T. Yamaguchi, F. Miyata, S.-I. Nakao, Polymer electrolyte membranes with a pore-filling structure for a direct methanol fuel cell, *Adv. Mater.* 15 (2003) 1198.
- [38] H. Munakata, D. Yamamoto, K. Kanamura, Properties of composite proton-conducting membranes prepared from three-dimensionally ordered macroporous polyimide matrix and polyelectrolyte, *Chem. Commun.* (2005) 3986.